

Nanostructured Cocrystals of a Borazine with [60]Fullerene

Simon Kervyn,¹ Takashi Nakanishi,^{*2} Junko Aimi,² Akinori Saeki,³ Shu Seki,³ Benoît Champagne,⁴ and Davide Bonifazi^{*1,5}¹Namur Research College (NARC) and Department of Chemistry, University of Namur (FUNDP), Rue de Bruxelles 61, 5000 Namur, Belgium²National Institute for Materials Science (NIMS), 1-2-1 Sengen, Tsukuba, Ibaraki 305-0047³Department of Applied Chemistry, Graduate School of Engineering, Osaka University, 2-1 Yamadaoka, Suita, Osaka 565-0871⁴Laboratory of Theoretical Chemistry, University of Namur (FUNDP), Rue de Bruxelles 61, 5000 Namur, Belgium⁵Department of Pharmaceutical and Chemical Sciences, University of Trieste, Piazzale Europa 1, 34127 Trieste, Italy

(Received May 14, 2012; CL-120562; E-mail: takashi.nakanishi@nims.go.jp, davide.bonifazi@fundp.ac.be)

In this paper, the preparation and photophysical characterization of nanostructured cocrystals composed of *B*-trimesityl-*N*-triphenylborazine (**1**) and C₆₀ are reported. Preliminary results in the solid state show that the borazine-centered fluorescence is quenched in the cocrystal, displaying strong interchromophoric interaction in the solid state, as also shown by photoconductivity measurements.

Being good electron acceptors,¹ [60]fullerene (C₆₀) and its derivatives show fascinating physical properties which display a huge potential for the development of new materials.² Among other characteristics, they have been shown to trap excited electrons efficiently and transfer them to the electrode, thus revealing these materials to make good molecular components for photovoltaics.³ For organic thin-layer solar-cell applications, classical values for the exciton diffusion length are in the range 10–20 nm, meaning that the electron donor (D) and acceptor (A) counterparts should be in a close arrangement. In this respect, bulk heterojunction organic solar cells have allowed an improvement in efficiency owing to their better charge-separation performances.⁴ However, for the achievement of reproducible and higher efficiencies, the photoactive architecture must possess a precisely controlled molecular organization.^{3a} In this respect, the supramolecular route can lead to self-organized materials with an appropriate D–A configuration at controlled distances.⁵ Among the different approaches, the cocrystallization of D and A molecular units in bulk heterosystems displaying predictable and tunable distances enabling charge-transfer interactions has shown to lead to materials that display very reproducible physicochemical properties.^{6,7} We recently synthesized a hexasubstituted borazine⁸ (**1**) (Figure 1a) bearing six aromatic rings, which displays a high extinction coefficient ($4 \times 10^3 \text{ M}^{-1} \text{ cm}^{-1}$ in CH₂Cl₂) in the UV region. As a first demonstration of the use of such hexasubstituted borazines in photoactive materials for photovoltaic applications, we report herein a study of the supramolecular organization between **1** and C₆₀ in the solid state, along with its photophysical measurements.

B-Trimesityl-*N*-triphenylborazine (**1**) was solubilized with an equimolar amount of pristine C₆₀ in *ortho*-dichlorobenzene. The solvent was evaporated by slow evaporation at room temperature (r.t.) to yield dark crystals (Figures 1b and S1¹⁵). Unfortunately, single-crystal X-ray diffraction analysis was

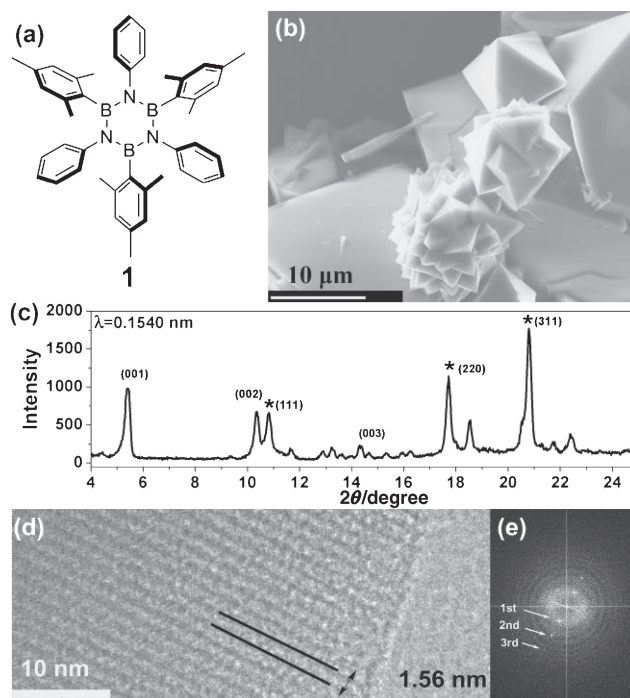


Figure 1. a) A chemical structure of *B*-trimesityl-*N*-triphenylborazine (**1**). b) SEM image of the cocrystal showing the crystal twinning of bipyramid. c) XRD of the cocrystal, *-marked peaks are the peaks of fcc C₆₀. d) HR-TEM image of the cocrystal showing the line arrangement of 1.56 nm width. e) The corresponding FFT analysis showing the 1st, 2nd, and 3rd order spots.

unable to determine the molecular organization in the solid state. In fact, several micrometer-sized bipyramidal crystals revealed the formation of crystal twinning, as observed by scanning electron microscopy (SEM, JEOL NeoScope JCM-5000) (Figure 1b). Therefore, the structure of the nanostructured cocrystals was investigated by means of powder X-ray diffraction (XRD, Rigaku RINT-2200HF Ultima), high-resolution transmission electron microscopy (HR-TEM, JEOL JEM-2100F, 200 kV), and solid-state UV–vis absorption spectroscopy.

As shown in Figure 1c, XRD confirmed that the obtainment of the cocrystal, the diffraction pattern being different from that

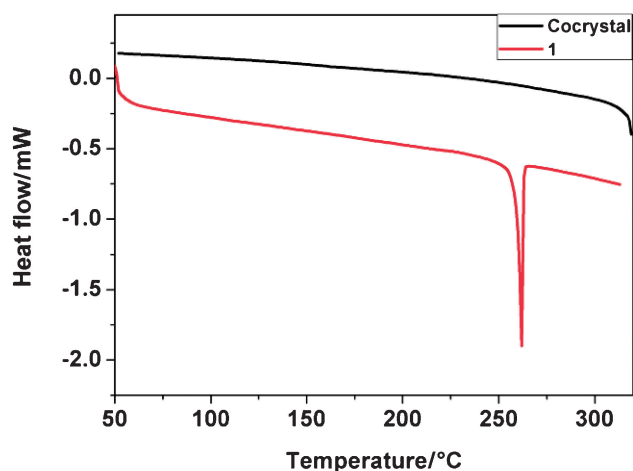


Figure 2. DSC profiles for 1:C₆₀ cocrystals (black) and **1** (red). The peak at 262 °C corresponds to the melting temperature of **1**. Clearly, this peak is absent in the cocrystal derivative.

of the classical fcc C₆₀ crystalline structure⁹ as well as from the borazine R $\bar{3}c$ crystal (Figure S2).¹⁵ The cocrystal pattern shows two main peaks at 5.4 and 10.5°, corresponding to *d* values of 1.60 and 0.84 nm, respectively. These peaks probably represent the layer structure from its (001) and (002) planes. However, small quantities of the segregate fcc C₆₀ crystal were also observed in the samples (marked * in Figure 1c). In addition, HR-TEM analysis of the nanostructures shows a periodic structure with a 1.56-nm layer distance (Figures 1d and S3¹⁵). The appearance of third-order spots in the fast Fourier transform (FFT) analysis indicates a certain degree of periodicity. In particular, the interlayer distance observed in the TEM results (1.56 nm) is in good agreement with the plane distance (1.60 nm) observed by XRD (Figure 1c).

Thermal analysis (TGA, Figures S4 and S5¹⁵) and DSC confirmed the effective cocrystallization of both molecules and the change of their physical properties as a consequence of their interaction. For example, in the DSC profile of the cocrystal (Figure 2), no melting-centered peak (at 262 °C, red curve of Figure 2) has been observed for the borazine counterpart, displaying a good homogeneity of the sample and the absence of free borazine in the sample. Occasionally, a peak at 181 °C in the first heat ramp has been also observed, corresponding to the evaporation of the remaining crystallization solvent, i.e., *ortho*-dichlorobenzene.

Further structural analysis is currently in progress, with the aim of understanding the precise molecular arrangement between **1** and C₆₀, and exploring different crystallization techniques for the preparation of suitable single crystals for X-ray diffraction analysis.

The UV–vis absorption spectrum of a 1:1 solution of **1** and C₆₀ in CH₂Cl₂ (Figure S6¹⁵) showed no additional features, thus indicating a ground-state charge transfer occurring between the two molecular species. The absorption spectrum of molecule **1** showed three bands at 272, 265, and 257 nm as well as a main peak at 230 nm (Figure S6). The steady-state UV–vis absorption spectrum of the cocrystal in the solid state (Figure 3a) reveals a pronounced tail up to 800 nm, possibly suggesting the occurrence of a charge-transfer process between C₆₀ and **1**, the latter

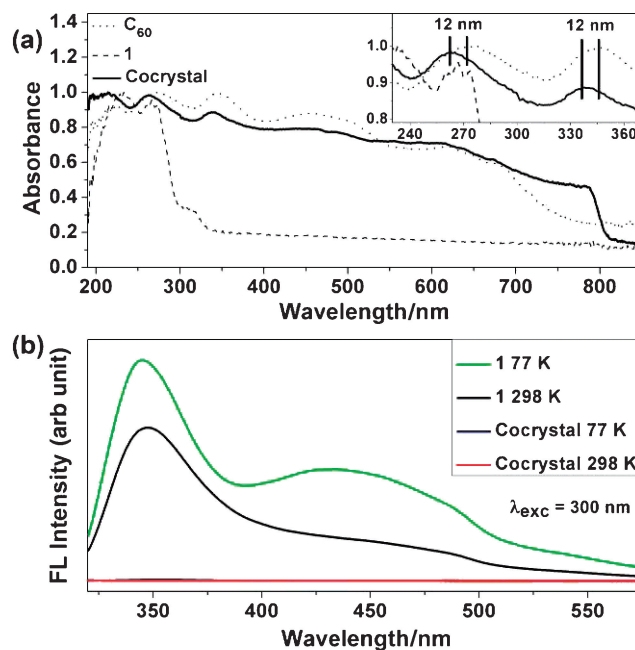


Figure 3. a) Solid-state UV–vis absorption spectra of **1** (dash), C₆₀ (dot), and the cocrystal (solid). b) Solid-state emission spectra of **1** at 298 (black) and 77 K (green) and of the 1:C₆₀ cocrystal at 298 (red) and 77 K (blue).

acting as an electron-donating species.¹⁰ Additionally, a 12-nm blue shift was observed for the fullerene-centered absorption peaks (at 271 and 346 nm) compared to those of crystalline C₆₀. This shift could be attributed to the attenuation of the π – π stacks between neighboring C₆₀ molecules¹¹ in the cocrystal, possibly due to the presence of intercalating borazine molecules.

Borazine derivatives are known to be efficient UV emitters in solution.¹² Molecule **1** has also been revealed to be a good UV emitter in the solid state, with a fluorescence peak maximum centered at 350 nm (Figure 3b). The measured absolute fluorescence quantum yield is approximately 13% at r.t., while at 77 K it increases to 22.9% with the appearance of a broad and novel emission band between 400 and 500 nm. On the contrary, no detectable emissive features have been observed for samples containing the 1:C₆₀ cocrystals (Figure 3b, red and blue lines). This suggests that a close spatial proximity, allowing strong interchromophoric interactions in the solid state, is adopted.

Finally, the charge-transport properties in the solid state of both borazine **1** alone and the 1:C₆₀ cocrystal were measured by time-resolved microwave conductivity (TRMC)¹³ (Figure 4). The measured transient photoconductivity ($\phi\Sigma\mu$ = the product of the quantum efficiency of the charge-carrier generation ϕ and the sum of the nanometer-scale charge-carrier mobilities, $\Sigma\mu = \mu_+ + \mu_-$) for the cocrystal ($1.55 \times 10^{-5} \text{ cm}^2 \text{ V}^{-1} \text{ s}^{-1}$) is three times higher than that of molecule **1** alone ($0.46 \times 10^{-5} \text{ cm}^2 \text{ V}^{-1} \text{ s}^{-1}$). Such enhanced photoconductivity values may be due to two factors: i) the intrinsic high photoconductivity of C₆₀, and/or ii) the increase in the ϕ value.¹⁴ A dramatic enhancement of ϕ would probably indicate the presence of additional photoinduced electron-transfer processes occurring between molecule **1** and C₆₀, which are attenuated in the segregate crystals of the molecular components. Notably, it can

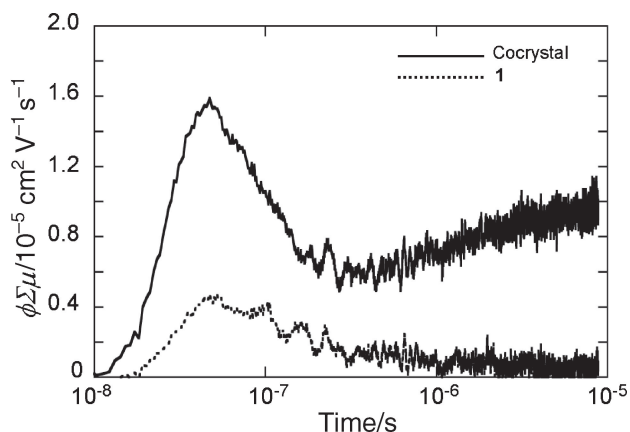


Figure 4. TRMC transient decay profiles of the cocrystal (solid) and powder of **1** alone (dot) under excitation at $\lambda = 355$ nm.

be observed that the lifetime of the charge-separated species (Figure 4) for the cocrystals displays higher values, thus indicating the presence of additional charge-separated states.

Theoretical investigations (as obtained by a DFT level of approximation using the M06 exchange-correlation functional and the 6-311G* basis set, Figures S7 and S8¹⁵) have shown that borazine **1** has a band gap of 5.8 eV and possesses appropriate HOMO and LUMO energy levels to allow photoinduced electron transfer from borazine to C₆₀. In fact, the borazine-centered LUMO is 3.1 eV higher than the LUMO of C₆₀ (Figure S7).

In conclusion, we have reported here the first evidence of interactions between a borazine derivative and C₆₀ in the crystalline solid state. The observed tendency for cocrystallization together with the decrease in luminescence intensity provides good evidence for a strong interchromophoric interaction in the solid state between the fullerene and borazine modules. We are now conducting a quantitative investigation of the photophysical properties in order to clarify, using time-dependent measurements in solution, whether or not the quenching of the luminescence derived from photoinduced energy-transfer and/or electron-transfer processes also results in covalent adducts.

DB, TN, and SK gratefully acknowledge generous support from the NIMS internship program and FNRS exchange grants. SK thanks FRIA for his doctoral fellowship. DB thanks the EU through the ERC Starting Grant COLORLANDS (contract 280183), FRS-FNRS (FRFC contracts n° 2.4.550.09 and 2.4.617.07.F and MIS n° F.4.505.10.F), the “Loterie Nationale,” the “TINTIN” ARC project (09/14-023), and the University of Namur and NARC (internal funding). The theoretical modeling was performed on the Interuniversity Scientific Computing Facility installed at the FUNDP, supported by the FRS-FRFC (Convention No. 2.4.617.07.F). We thank JASCO for technical support for low-temperature fluorescence measurements and Dr. M. Takeuchi (NIMS) for useful discussions.

Paper based on a presentation made at the International Association of Colloid and Interface Scientists, Conference (IACIS2012), Sendai, Japan, May 13–18, 2012.

References and Notes

- a) D. Bonifazi, A. Kiebele, M. Stöhr, F. Cheng, T. Jung, F. Diederich, H. Spillmann, *Adv. Funct. Mater.* **2007**, *17*, 1051. b) Q. Xie, E. Pérez-Cordero, L. Echegoyen, *J. Am. Chem. Soc.* **1992**, *114*, 3978. c) T. Nakanishi, H. Ohwaki, H. Tanaka, H. Murakami, T. Sagara, N. Nakashima, *J. Phys. Chem. B* **2004**, *108*, 7754.
- a) F. Diederich, M. Gómez-López, *Chem. Soc. Rev.* **1999**, *28*, 263. b) A. M. López, A. Mateo-Alonso, M. Prato, *J. Mater. Chem.* **2011**, *21*, 1305. c) D. Bonifazi, O. Enger, F. Diederich, *Chem. Soc. Rev.* **2007**, *36*, 390. d) D. M. Guldi, B. M. Illescas, C. M. Atienza, M. Wielopolski, N. Martín, *Chem. Soc. Rev.* **2009**, *38*, 1587. e) T. Nakanishi, *Chem. Commun.* **2010**, *46*, 3425. f) S. S. Babu, H. Möhwald, T. Nakanishi, *Chem. Soc. Rev.* **2010**, *39*, 4021.
- a) T. M. Clarke, J. R. Durrant, *Chem. Rev.* **2010**, *110*, 6736. b) H. Imahori, *J. Phys. Chem. B* **2004**, *108*, 6130.
- P. W. M. Blom, V. D. Mihailetschi, L. J. A. Koster, D. E. Markov, *Adv. Mater.* **2007**, *19*, 1551.
- L. Schmidt-Mende, A. Fechtenkötter, K. Müllen, E. Moons, R. H. Friend, J. D. MacKenzie, *Science* **2001**, *293*, 1119.
- a) Y. Shibano, H. Imahori, C. Adachi, *J. Phys. Chem. C* **2009**, *113*, 15454. b) T. Wakahara, P. D’Angelo, K. Miyazawa, Y. Nemoto, O. Ito, N. Tanigaki, D. D. C. Bradley, T. D. Anthopoulos, *J. Am. Chem. Soc.* **2012**, *134*, 7204.
- L. Wei, Y. Wu, L. Wang, H. Fu, J. Yao, *J. Phys. Chem. C* **2011**, *115*, 21629.
- S. Kervyn, O. Fenwick, F. Di Stasio, Y. Sig Shin, J. Wouters, S. Osella, D. Beljonne, G. Accorsi, N. Armaroli, F. Cacialli, D. Bonifazi, unpublished results.
- a) K. Miyazawa, Y. Kuwasaki, A. Obayashi, M. Kuwabara, *J. Mater. Res.* **2002**, *17*, 83. b) X. Zhang, M. Takeuchi, *Angew. Chem., Int. Ed.* **2009**, *48*, 9646.
- T. Wakahara, M. Sathish, K. Miyazawa, C. Hu, Y. Tateyama, Y. Nemoto, T. Sasaki, O. Ito, *J. Am. Chem. Soc.* **2009**, *131*, 9940.
- T. Nakanishi, H. Murakami, N. Nakashima, *Chem. Lett.* **1998**, 1219.
- A. Wakamiya, T. Ide, S. Yamaguchi, *J. Am. Chem. Soc.* **2005**, *127*, 14859.
- A. Saeki, S. Seki, T. Takenobu, Y. Iwasa, S. Tagawa, *Adv. Mater.* **2008**, *20*, 920.
- a) X. Zhang, T. Nakanishi, T. Ogawa, A. Saeki, S. Seki, Y. Shen, Y. Yamauchi, M. Takeuchi, *Chem. Commun.* **2010**, *46*, 8752. b) S. S. Babu, A. Saeki, S. Seki, H. Möhwald, T. Nakanishi, *Phys. Chem. Chem. Phys.* **2011**, *13*, 4830.
- Supporting Information is available electronically on the CSJ-Journal Web site, <http://www.csj.jp/journals/chem-lett/index.html>.